CHAPTER 4

POLARIZATION RECOMBINING SCHEME: PRINCIPLE AND POLARIZATION CHARACTERISTICS MEASUREMENTS

4.1. Introduction

In the previous chapter, three main approaches to solving the fluctuations in the SOP of the received signal in coherent optical fiber communications have been reviewed; these are classified as (1) use of a polarization-maintaining fiber in the signal lightguide, (2) use of polarization insensitive receivers, and (3) use of SOP control devices. In an SOP device, the most important characteristic to be realized is, no need for "resetting" for any type of SOP change in the coming signal. So far, the endlessness (resetting-free) in control has been achieved by only two methods: the rotatable phase-plate scheme [89] and the rotatable fiber crank scheme [90].

In this thesis, a new endless (resetting-free) SOP control scheme called "polarization recombining" which features a very simple (probably the simplest) principle for the SOP control is proposed. In addition, the SOP of the output light from the system is always linear with a fixed inclination angle. This chapter describes the principle and presents some experimental results of such scheme.

4.2. Principle

The principle idea of the polarization recombining scheme is shown in Fig.23. An arbitrary polarized light at the fiber exit is separated into two orthogonal linearly polarized lights (i.e. a vertical V: and a horizontal (H:)) by a polarization beam splitter such as a Wollaston prism. The horizontal component is converted to a vertical one by rotating its polarization plane by 90° using a linear polarization rotator (a half-wave plate (HWP)), and then recombined with the vertical component in a half-mirror. The interfering output intensities I_1 and I_2 at the half-mirror output ports 1 and 2, respectively, are given as

$$I_1 \propto I_h + I_v + 2\sqrt{I_h I_v}\cos\phi \tag{34}$$

$$I_2 \propto I_h + I_v - 2\sqrt{I_h I_v}\cos\phi \tag{35}$$

$$\phi = \gamma_{hv} - \alpha \tag{36}$$

where I_h and I_v are, respectively the amplitudes of the H: and V: components, ϕ is the phase difference between the two arms of the interferometer, γ_{hv} is the relative phase difference between the two components, and α is

the additional phase shift induced by the endless phase shifter.

4.2.1. Type-I polarization recombining scheme

The schematic diagram of this type is shown in Fig. 23(a). When the phase difference ϕ between the two arms of the interferometer is $m\pi/2$ ($m = \pm1, \pm3, \pm5,...$), the output intensities at ports 1 and 2 will be equal (i.e. $I_1 = I_2 = I_h + I_v$) regardless of the different relative intensities in the two arms. The SOP's of the two output lights are the same and always linear with a fixed inclination angle determined by the principal axis of the Wollaston prism regardless of changes in the SOP of the input signal light. In this scheme, therefore, the phase shift given by the endless phase shifter is adjusted so that the output intensities at ports 1 and 2 detected by the photodetectors P1 and P2, respectively, are equal.

4.2.2. Type-II polarization recombining scheme

Figure 23(b) shows the schematic diagram of this type. From eq.(34) and eq.(35), it can be seen that the maximum ($I_{max} = 4I_h$ or $4I_v$) and the minimum ($I_{min} = 0$) interfering outputs at ports 1 and 2, respectively, are obtainable when $\phi = 2m\pi$ (m: integer) and $I_h = I_v$. In this scheme, therefore, the polarization inclination angle given to the signal light by the polarization

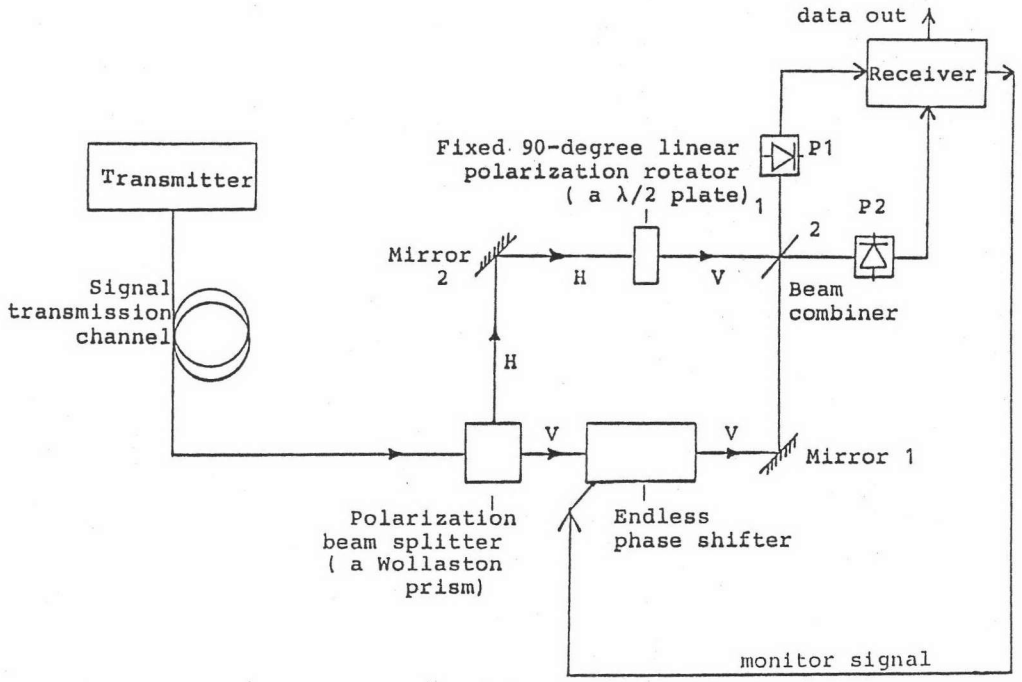

(a)

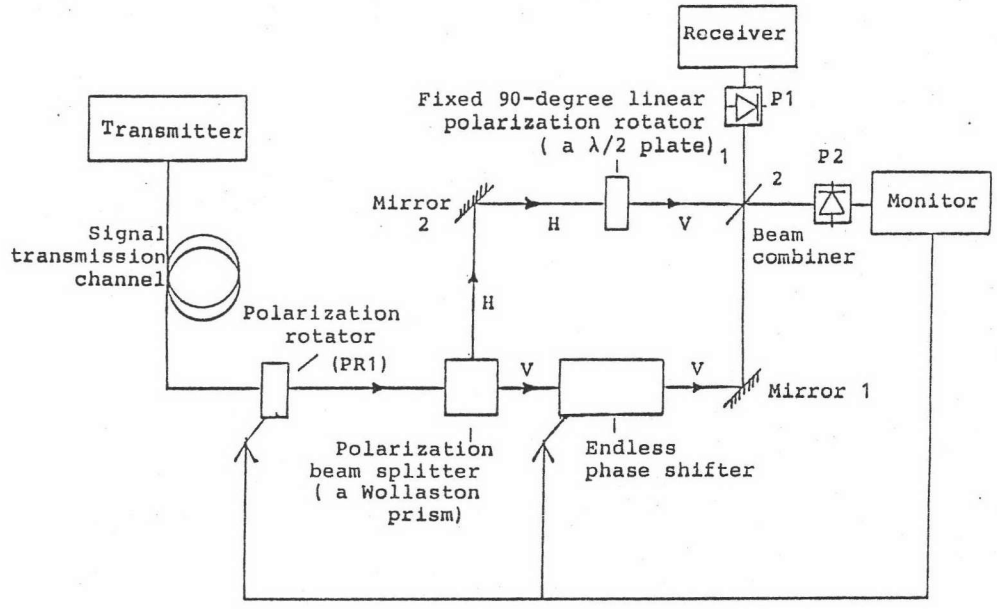

(b)

Fig. 23. Type-V SOP control scheme, (a) Type-I Polarization recombining scheme; (b) Type-II Polarization recombining scheme, (present work, see text for details).

rotator and the phase shift given by the endless phase shifter are adjusted so that the input to the monitor branch 2 is minimized.

The key component in these schemes is the endless phase shifter which will be discussed latter in Chapter 5. In the following sections, results on polarization characteristics measurements of the output light from a polarization recombining circuit are presented.

4.3. Polarization characteristics measurements

4.3.1. Principle of measurements

a) visibility:

Let I_h and I_v are the light intensities of the horizontal (H:) and vertical (V:) components, respectively. According to [32], the photocurrents at the output ports 1 and 2 resulting from the interference of the two beams can be expressed as

$$I_1 = R(kI_h + (1-k)I_v + 2\sqrt{k(1-k)I_hI_v}\, u_{hv}(\tau)\cos(\gamma_{hv}-\delta)) \tag{37}$$

$$I_2 = R(kI_h + (1-k)I_v - 2\sqrt{k(1-k)I_hI_v}\, u_{hv}(\tau)\cos(\gamma_{hv}-\delta)) \tag{38}$$

$$\phi = \gamma_{hv} - \delta \tag{39}$$

where R is the photodetectors' responsivity, τ and u_{hv} denote the group delay time difference between the two orthogonal components and degree of coherence, respectively, k is the transmitivity of a half-mirror, γ_{hv} is the phase difference between the two components, δ and is the additional phase corresponding to the phase shift induced by the PZT-mounted mirror.

The intensity maxima and minima are given by

$$I_1(max,min) = R(kI_h + (1-k)I_v \pm 2\sqrt{k(1-k)I_hI_v}\,u_{hv}(\tau)) \quad (40)$$

$$I_2(max,min) = R(kI_h + (1-k)I_v \pm 2\sqrt{k(1-k)I_hI_v}\,u_{hv}(\tau)) \quad (41)$$

where the upper sign is for $\phi = m\pi$ ($m = 1, 3, 5, \ldots$) and the lower sign is for $\phi = m\pi$ ($m = 0, 2, 4, \ldots$). Hence, the visibility [32] is defined as

$$V = (Imax - Imin)/(Imax + Imin) \quad (41)$$

when $I_h = I_v$ and $k = 1/2$, eq.(41) reduces to

$$V = u_{hv}(\tau) \quad (42)$$

For completely coherent superposition $u_{hv}(\tau) = 1$, partially coherent superposition $0 < u_{hv}(\tau) < 1$, and

incoherent superposition $u_{hv}(\tau) = 0$.

The intensity factor (IF) is defined as

$$IF = IF_1/(IF_1 + IF_2), \text{ or } IF = IF_2/(IF_1 + IF_2) \tag{43}$$

From eq.(41) and eq.(43), the relationships between the intensity factor and the visibility can be expressed as

$$V = 2IF_1 - 1, \text{ or } V = 2IF_2 - 1 \tag{44}$$

Variation of photocurrents with phase difference ϕ for $k = 1/2$ and $I_h = I_v$ is illustrated in Fig. 24.

b) Polarization characteristics:

Consider the intensity of the recombined light passing through a polarizer with orientation angle θ and a quarter-wave plate (hereafter QWP) which introduces a phase difference of $\varepsilon = \pi/2$ between the orthogonally polarized components. I_1 becomes [32]

$$I_1(\theta,\varepsilon) = \frac{1}{2}J_{xx}\cos^2\theta + \frac{1}{2}J_{yy}\sin^2\theta + \sqrt{J_{xx}J_{yy}\cos\theta\sin\theta}\, u_{hv}(\tau)\cos(\phi-\varepsilon) \tag{45}$$

where, the transmittivity k of the half-mirror is assumed to be polarization independent and equal to 1/2, and J denotes the coherency matrix of the light (see Chapter 2).

According to [32], the strokes' parameters (S_0,

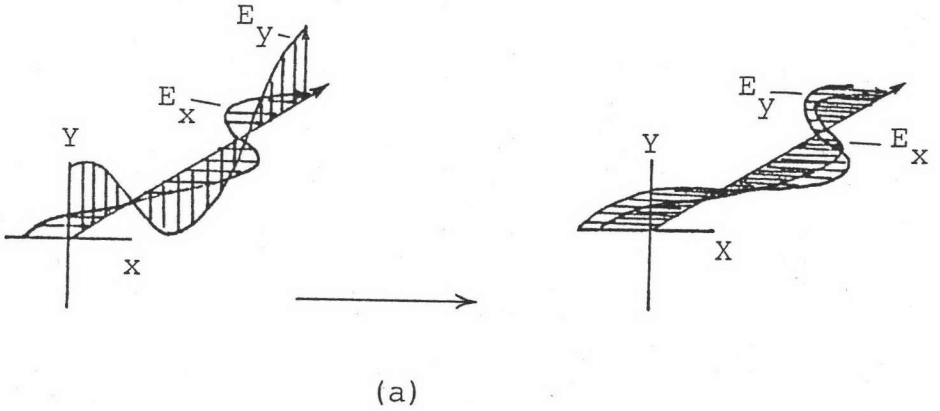

(a)

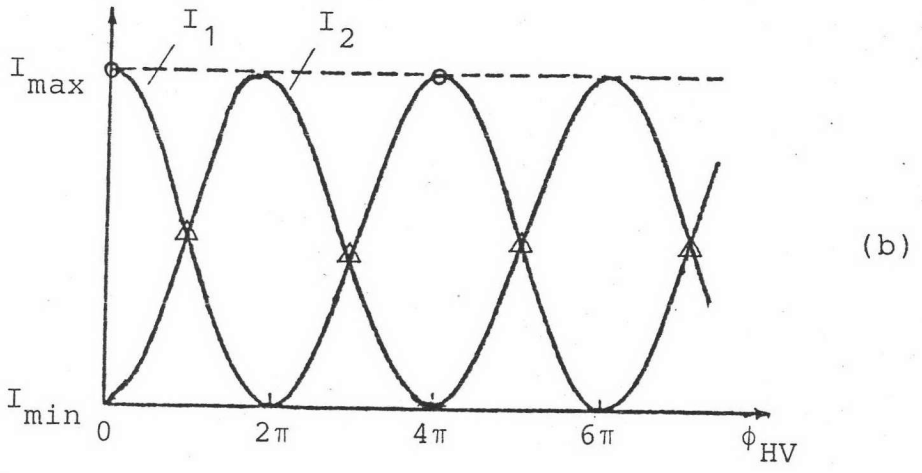

(b)

Fig. 24. Principle of polarization recombining scheme. (a) Interference of two orthogonal components when their polarization planes are parallel. (b) Variation of intensities with phase difference for equal intensity of the two orthogonal components; Δ - operating point for the Type-I polarization recombining scheme; o - operating point for the Type-II polarization recombining scheme.

S_1, S_2, S_3) used to characterize the SOP of a polarized light and the elements of the coherency matrix are related by the following formula :

$$\begin{aligned} S_0 &= J_{xx} + J_{yy} \\ S_1 &= J_{xx} - J_{yy} \\ S_2 &= J_{xy} + J_{yx} \\ S_3 &= i(J_{yx} + J_{xy}) \end{aligned} \tag{46}$$

The four Strokes' parameters can be determined from measurements of the intensity I_1 through various orientations of the polarizer such that

$$\begin{aligned} S_0 &= I_1\,(0°,0°) + I_1\,(90°,0°) \\ S_1 &= I_1\,(0°,0°) - I_1\,(90°,0°) \\ S_2 &= I_1\,(45°,0°) - I_1\,(-45°,0°) \\ S_3 &= I_1\,(225°,\pi/2) - I_1\,(135°,\pi/2) \end{aligned} \tag{47}$$

Hence, according to eq.(31) in Chapter 2, the DOP of the recombined light in terms of the strokes' parameters, is

$$P = I_{pol}/I_{tot} = \sqrt{(S_1^2 + S_2^2 + S_3^2)}/S_0 \tag{48}$$

where I_{tot} is the total intensity of the polarized part and I_{pol} is the total intensity of the recombined light.

The ellipticity χ ($-\pi/4 < \chi < \pi/4$) can be obtained as

$$\chi = 0.5*\sin^{-1}\left[S_3/\sqrt{(S_1^2 + S_2^2 + S_3^2)}\right] \tag{49}$$

and the inclination angle ψ ($0 < \psi < \pi$) is given by

$$\psi = 0.5*\mathrm{TAN}^{-1}\left(S_2/S_1\right) \tag{50}$$

The absolute maxima and minima (with respect to both θ and ε) intensities are

$$I,(MAX,MIN),(\theta,\varepsilon) = S_0/2\left[1 \pm \sqrt{1-(S_0-S_1-S_2-S_3)/S_0}\right] \tag{51}$$

$$I,(MIN,MAX),(\theta,\varepsilon) = S_0/2\left[1 \mp \sqrt{1-(S_0-S_1-S_2-S_3)/S_0}\right] \tag{52}$$

The linear polarization ratio Lp, which determines linearity of the recombined light is defined as

$$Lp = \sqrt{(S_1^2 + S_2^2)/(S_1^2 + S_2^2 + S_3^2)} \tag{53}$$

The extinction ratio η is defined as

$$\eta = 10*\log[Imax(\theta,\varepsilon)/Imin(\theta,\varepsilon)] \tag{54}$$

The power restoring factor γ is defined as

$$\gamma = Imax(\theta,\varepsilon)/[Imax(\theta,\varepsilon) + Imin(\theta,\varepsilon)] \tag{55}$$

It should be noted that the above expressions are usually used to characterize the polarization properties of a single beam of quasi-monochromatic (partially polarized) light which consists of two mutually orthogonal polarized components. In the present case, we have the interference of two linearly polarized light whose planes of polarization are parallel, so that either the H: component (I_h, 0) becomes (0, I_h) or the V: component (0, I_v) becomes (I_v, 0). This means that the orthogonal relationship between these two components vanishes, and the recombined beam is linearly polarized either in the x or y direction (perpendicular to the propagation direction z) depending on which component has its polarization plane rotated by 90°. Thus, the above method of determining the SOP can be applied to this particular case, since the two components are originated from the same source and the optical path difference introduced between the interfering beams can be made small compared to the coherence length $c/\Delta\nu$ of the light source, where c is the light velocity and $\Delta\nu$ is the effective linewidth.

4.3.2. Experimental set-up

The experimental set-up for measuring the visibility is shown in Fig. 25. Different lengths (300 m, 1.5 km., 15.4 km., and 27 km.) of single mode optical fibers are used and the parameters of these fibers are tabulated in Table III. Glan-Thomson polarizer P makes sure that light transmitted from a temperature stabilised 1.35 μm DFB laser is perfectly linearly polarized. The linearly polarized light is then converted to an arbitrary elliptically polarized one using a Babinet-Soleil compensator (BSC). The Wollaston prism (WP) separates the elliptically polarized light into two orthogonal components having a horizontal (H:) and a vertical (V:) linear polarization The H: component is then rotated by 90° using a HWP and latter combined with the V: component in a half-mirror (HM). The output interference intensities at port 1 and 2 are detected by the Ge-APD photodetectors PD1 and PD2, respectively, followed by electronic processing circuits.

The experimental set-up for polarization characteristics measurements is similar to that of the visibility measurement except that the photodetectors are alternatively replaced by an automatic polarization measuring system (a polarimeter) consisting of rotating analyzers and rotating QWP's

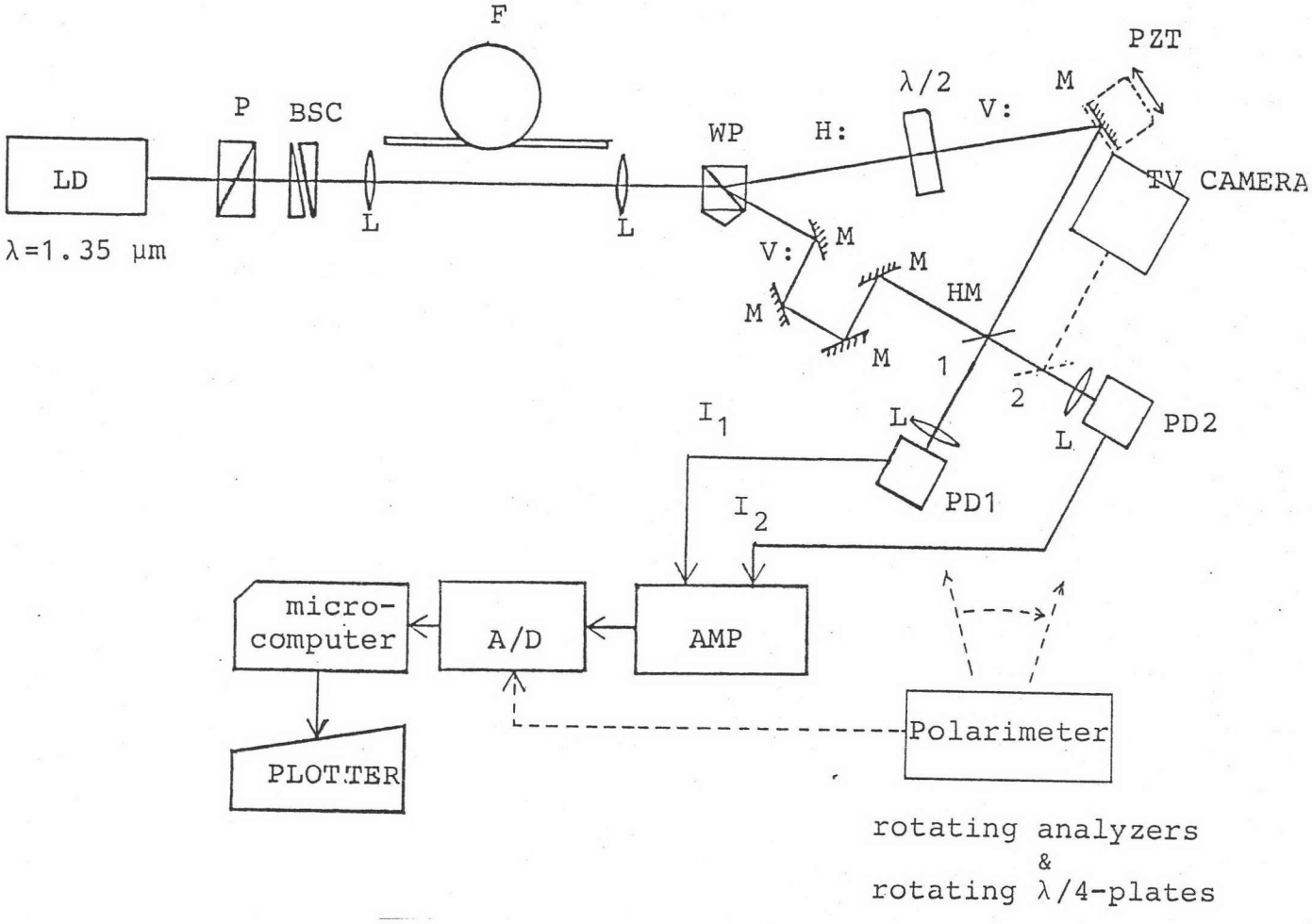

Fig. 25. Experimental setup of polarization recombining scheme for visibility and polarization characteristics measurements. LD : laser diode; P :Glan-Thompson polarizer; BSC :Babinet-Soleil compensator; L : lens; WP : Wallaston prism; M: mirror; HM : Half-mirror; PD : Ge-APD photodetector.

Table III. Fiber Parameters

Parameter			
Length [m]	1500	15410	27038
Loss [dB/km] (at 1.3 μm)	1.5	0.40	0.42
Cutoff frequency [μm]	0.83	1.23	1.21
Core diameter [μm]	6.6	9.35	8.73
Cladding diameter [μm]	150	125	124

4.3.3. Results and discussions

Photo. 1 shows the photographs of the fringe patterns obtained for unaligned and aligned polarization planes of the interfering beams using a silicon camera.

Figure 26 illustrates the variation of the photocurrents (I_1 and I_2) and visibility V as a function of PZT driving voltage Vd. It was found that the output currents varied sinusoidally and the visibility varied periodically. These results confirm that the quasi-monochromatic theory is valid for the interference property of the polarization recombining scheme. The maximum visibility for $I_h = I_v$ and $\phi = 0$ is 8.4 which is the value of the degree of coherence. This value was less than unity because two interfering beams were partially coherent. A linear relationship between the PZT driving voltage and its induced-phase shift was found, with an inclination of 5.4 deg./volt, as shown in Fig. 27.

Figure 28 shows the variation of polarization characteristics as a function of PZT driving voltage. The fluctuation of DOP within ± 0.09 from the mean value of 0.95 was due to the phase drift between the two interfering beams. However, the fluctuation could be worse if the phase compensation was not used in the measuring system.

The variation of SOP as a function of BSC rotation

angle is shown in Fig. 29. High DOP (around 0.96 for both with and without fiber) is preserved through difference rotation angles. The SOP of the recombined light was found to be linear with a fixed deflection (inclination) angle of -45°.

The SOP was found to degrade periodically every 90° when the polarizer and the BSC were exchanged their places, as shown in Fig. 30. This was due to the dependent of light intensity with the BSC rotation angle. The intensity was minimum at rotation angle of 45° and 135°. The chaotic of SOP can be observed in Fig. 31 and this was partly due to the intensity being below the minimum detectability of the polarimeter.

When the BSC was placed in front of the polarimeter the deflection angle was found to be rotated through 360° (see Fig. 32). This measurement was performed to demonstrate that the orthogonallity between the H: and V: components vanish.

A high DOP (= 0.82, see Fig. 33(b)) in the 27-km-long fiber was preserved and independent of the incident condition. However, the DOP decreased considerably in comparison with that in the 1.5-km-long fiber (DOP = 0.93, see Fig. 33(a)) and the 300-m-long fiber (DOP = 0.96, see Fig. 29(b)).

Figures 34(a) and (b) show that the inclination angle of the recombined light is 45° when the polarization plane of the V: component has been rotated

by 90°, and is -45° when the polarization plane of the H: component has been rotated by 90°, for 15.4-km test fiber. The DOP is about 0.88.

The polarization characteristics and output intensity fluctuation observed for 1 hr. are shown in Fig. 35(a) and (b) for the 15.4-km and 27-km-long fibers, respectively. In these figures, it is found that variations of the DOP, the ellipticity, the deflection angle, and the intensity fluctuation for the 15.4-km and 27-km-long fibers are within ±0.43, ±0.56, and ±4.4, ±5.2, and ±5.3, ±5.7, and ±2.1 dB, and ±2.12 dB, respectively. The slightly decrease in the DOP for both fibers with time was due to the thermal-drifting in offset-voltages of the amplifiers used in the polarimeter circuit, and the DOP fluctuation was due to random coupling in the fibers and randomness nature of the DOP.

Figures 36(a) and (b) indicate that the SOP's at both output ports 1 and 2 are matched regardless of the intensity levels when the measurements of SOP were carried out.

Residual unpolarized light which originated in the optical components; fiber cladding modes, mirrors, and polarizer and analyzer scattering also caused the variations in the SOP. The other source of error could be that the measurement of the four Strokes' parameters were not simultaneous. It took about 40 ms. to measure

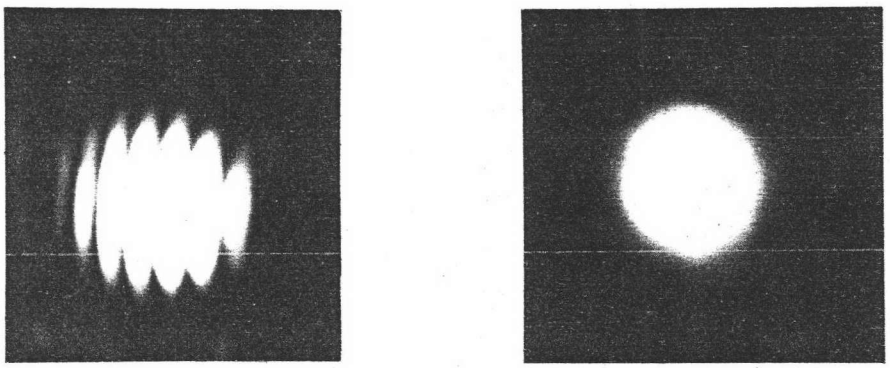

(a) (b)

Photo. 1. Fringe patterns obtained from a silicon video camera : (a) misaligned beams; (b) aligned beams.

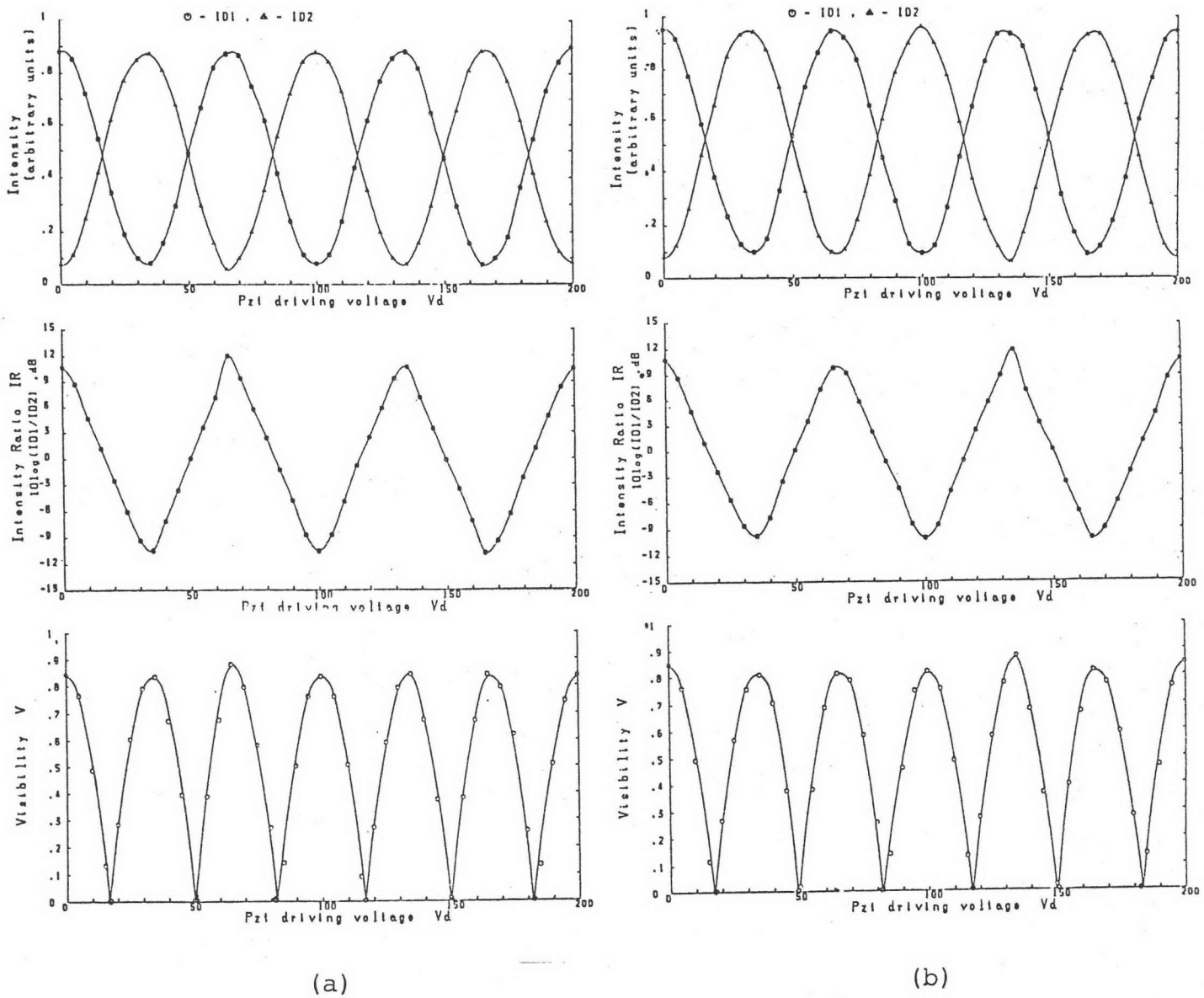

Fig.26.1. Variations of intensity, intensity ratio IR, and visibility V as a function of PZT driving voltage V_d. (a) without fiber; (b) with 300-m-long single-mode fiber.

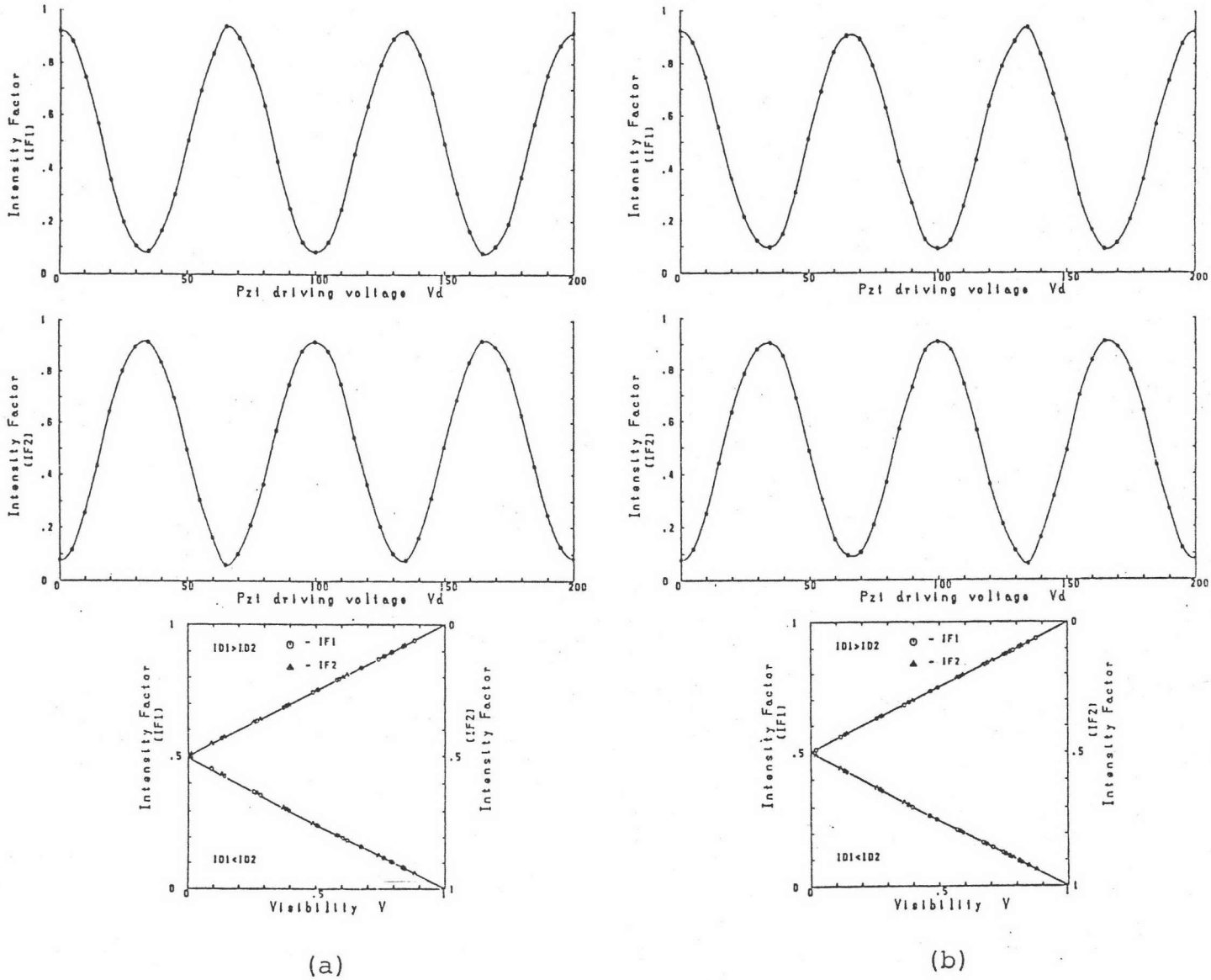

Fig. 26.2. Intensity factor IF_1, IF_2 VS PZT driving voltage V_d, and intensity IF_1, IF_2 VS visibility V : (a) without fiber; (b) with 300-m-long single-mode fiber.

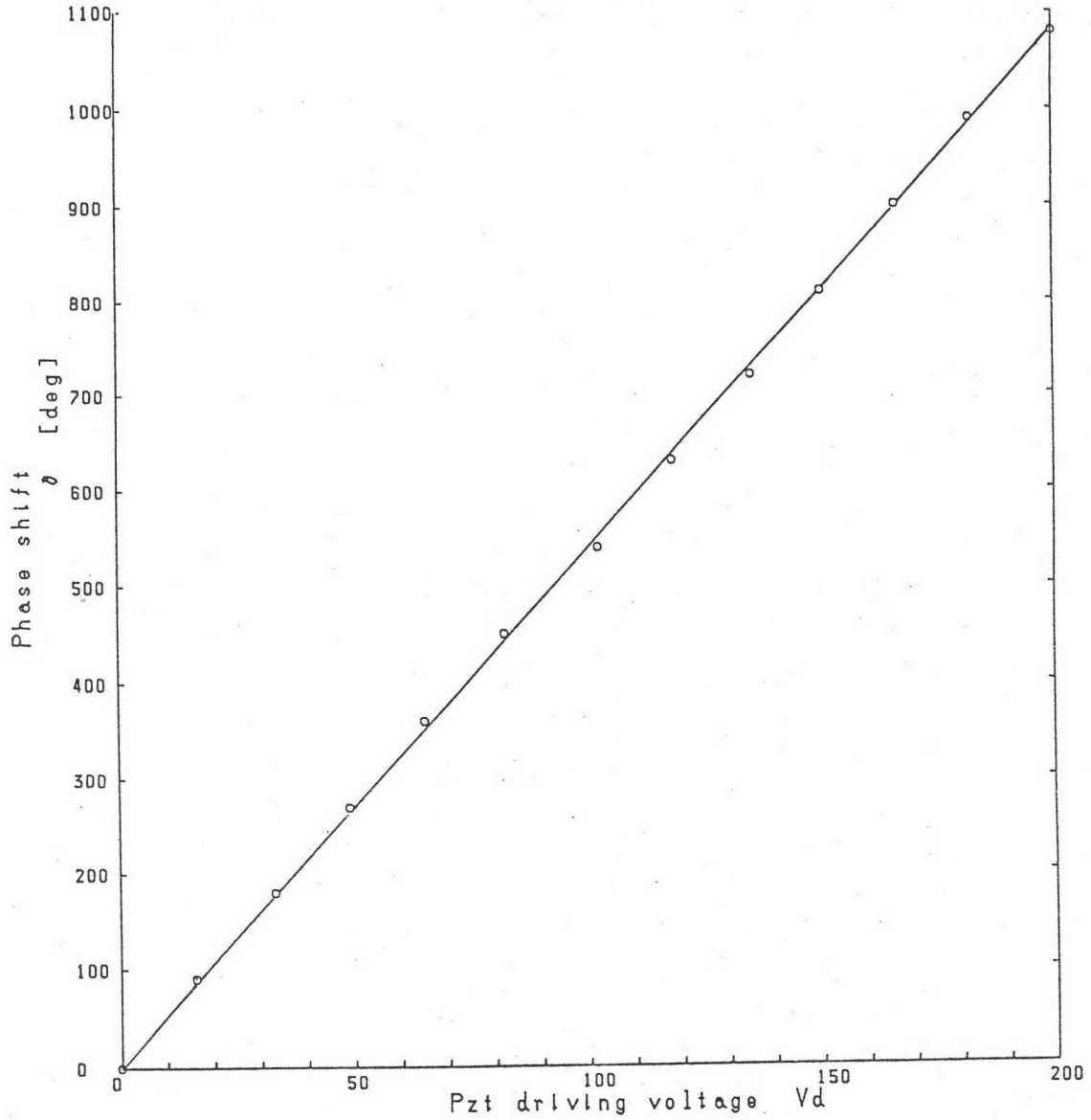

Fig. 27. Linear relationship between PZT-induced phase shift δ and PZT driving voltage V_d.

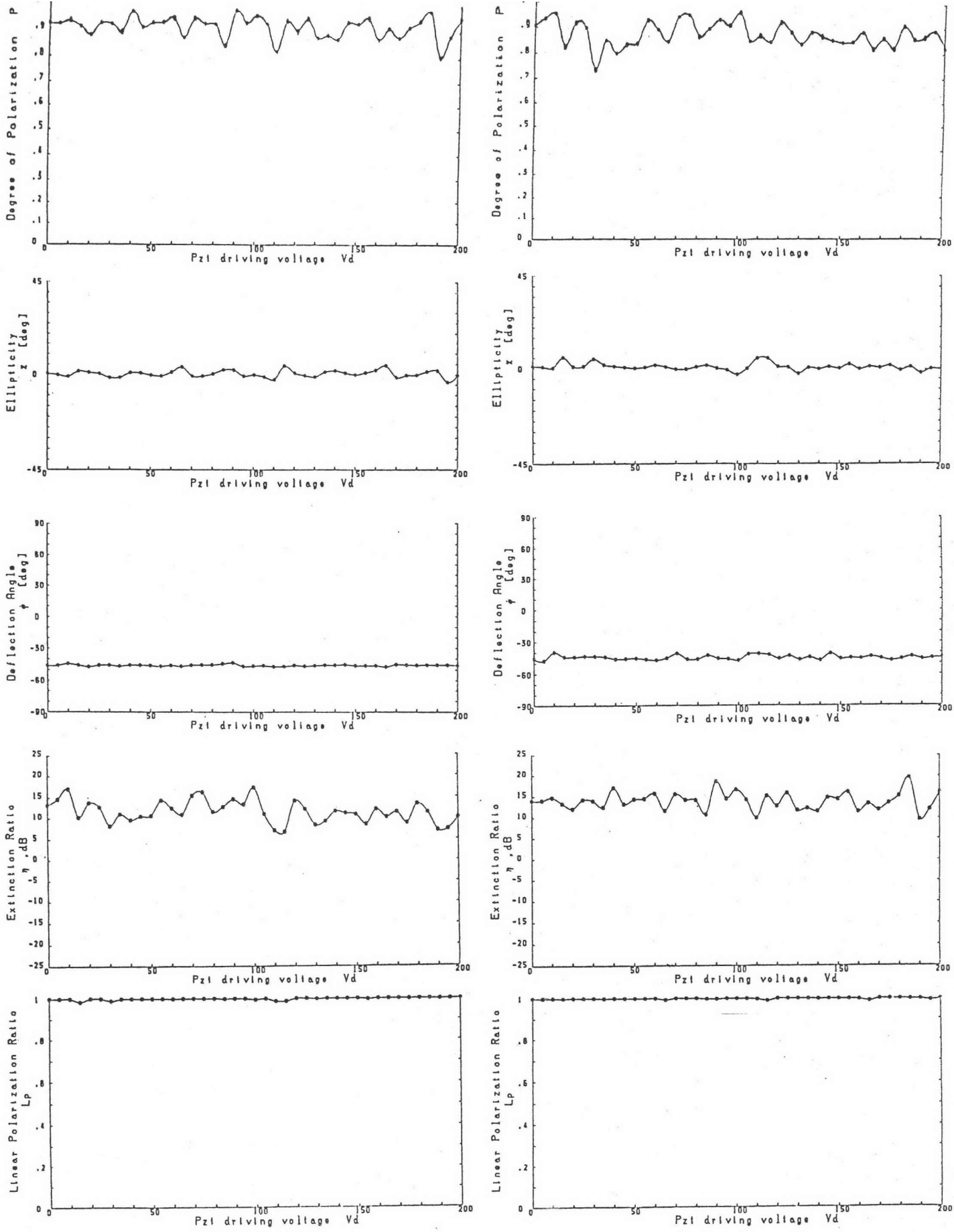

Fig. 28. Polarization characteristics of polarization recombined light as a function of PZT driving voltage V_d : (a) without fiber; (b) with 300-m-long single-mode fiber.

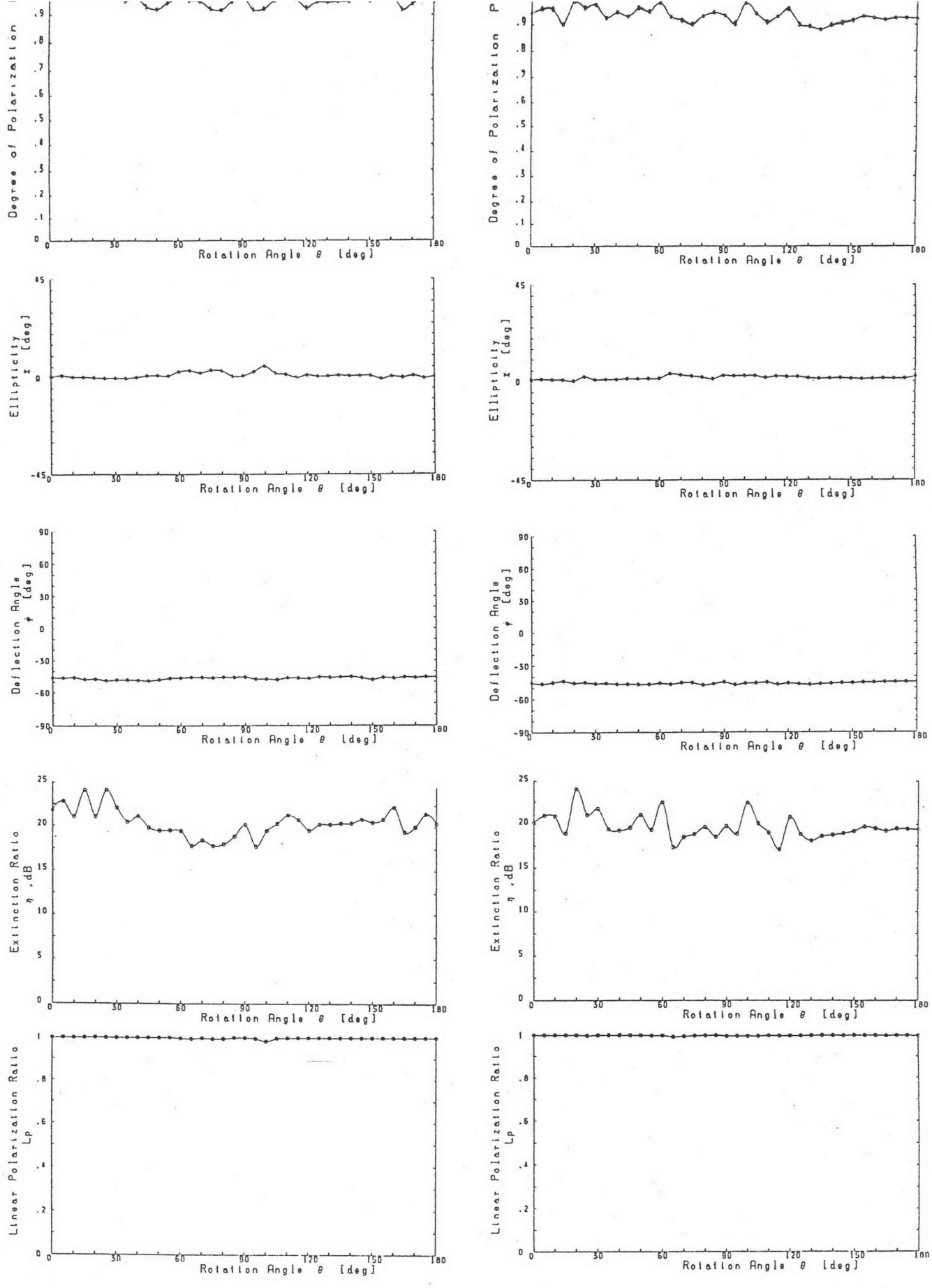

(a) (b)

Fig. 29. Polarization characteristics of polarization recombined light as a function of the BSC rotation angle : (a) without fiber; (b) with 300-m-long single-mode fiber.

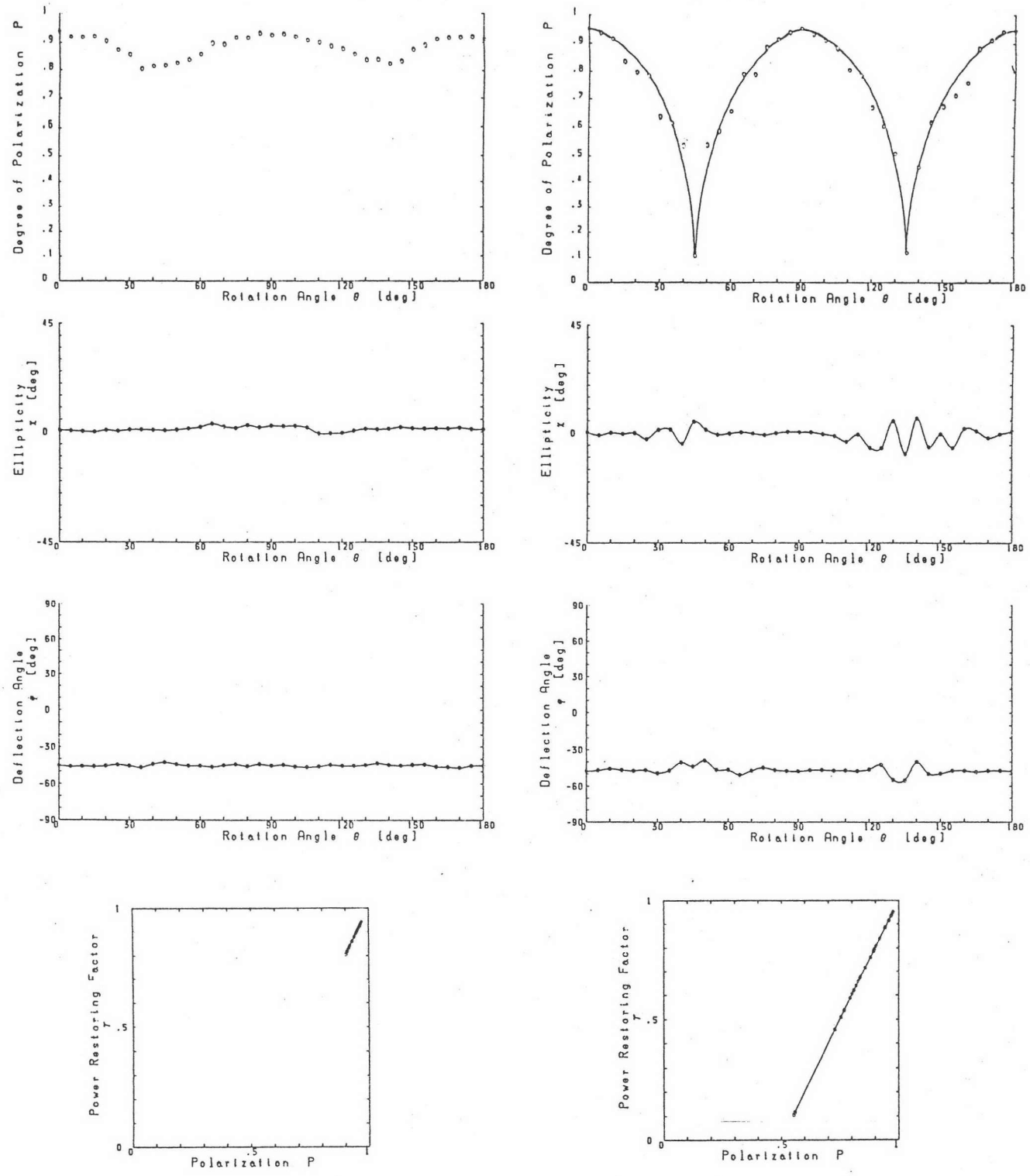

Fig. 30. Polarization characteristics of polarization recombined light as a function of the BSC rotator angle (when it was exchanged its place with P: (a) without fiber; (b) with 300-m-long single-mode fiber.

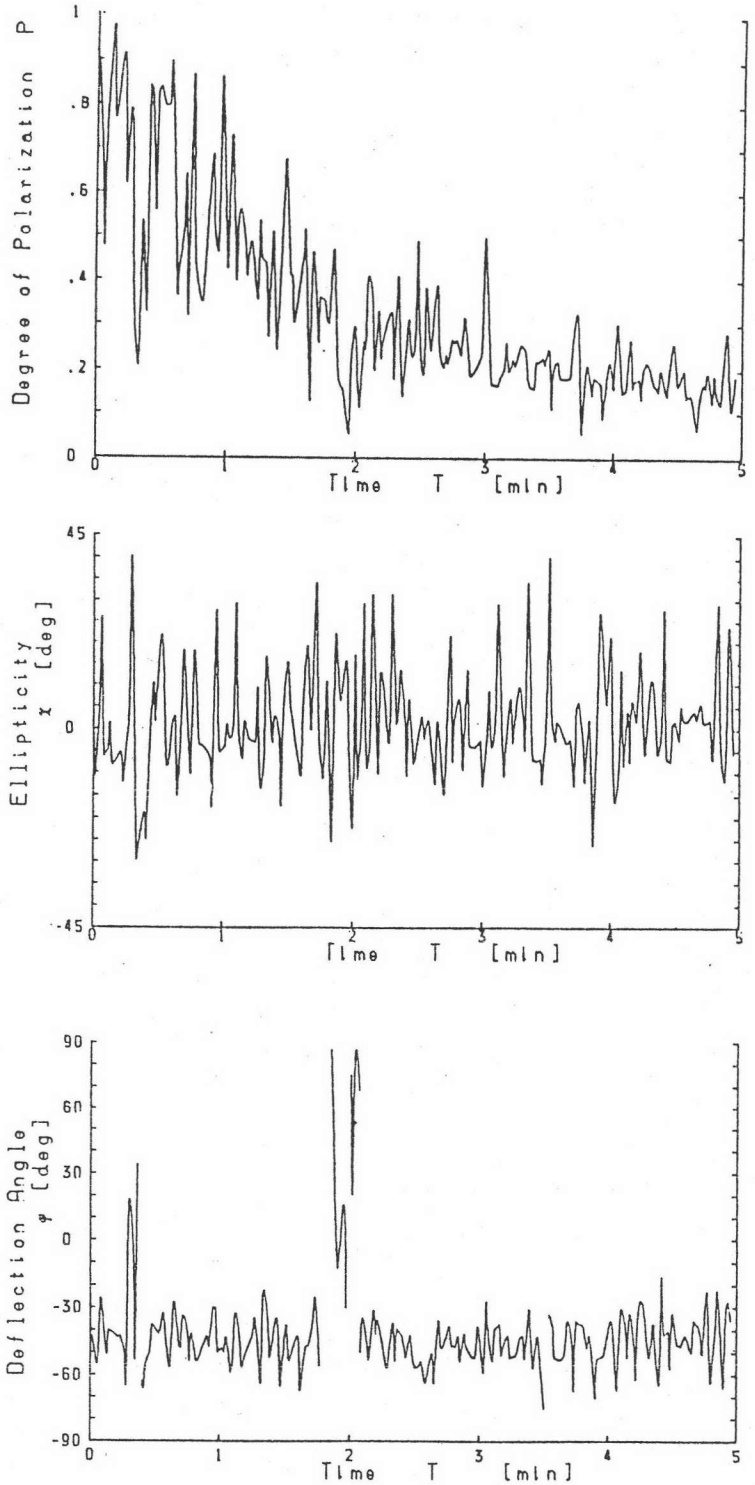

Fig. 31. Chaotic of polarization characteristics resulted from low intensity detected by the polarimeter (for 300-m-long single-mode fiber).

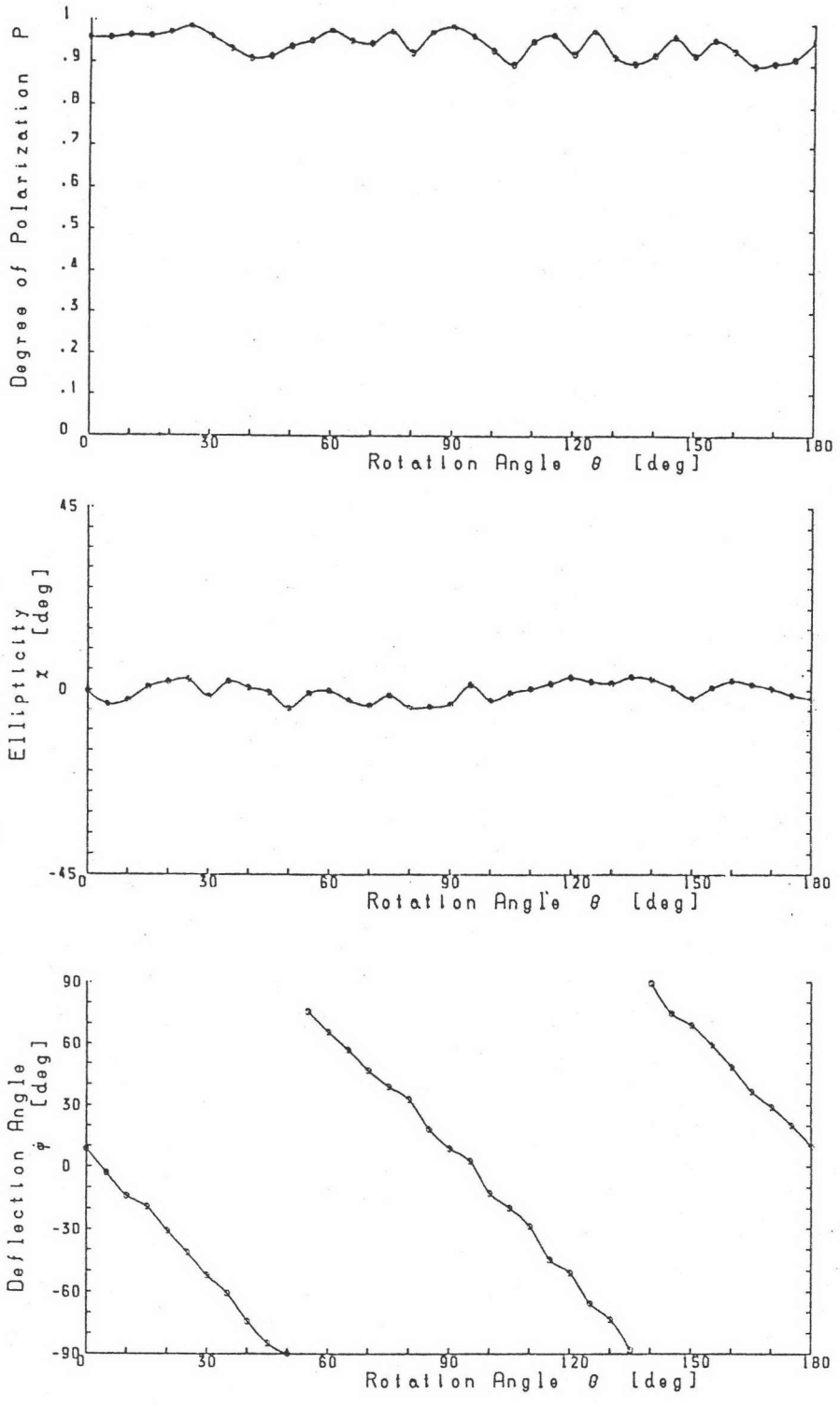

Fig. 32. Polarization characteristics of polarization recombined light as a function of the BSC rotation angle when it was placed in front of the polarimeter (for 300-m-long single-mode fiber).

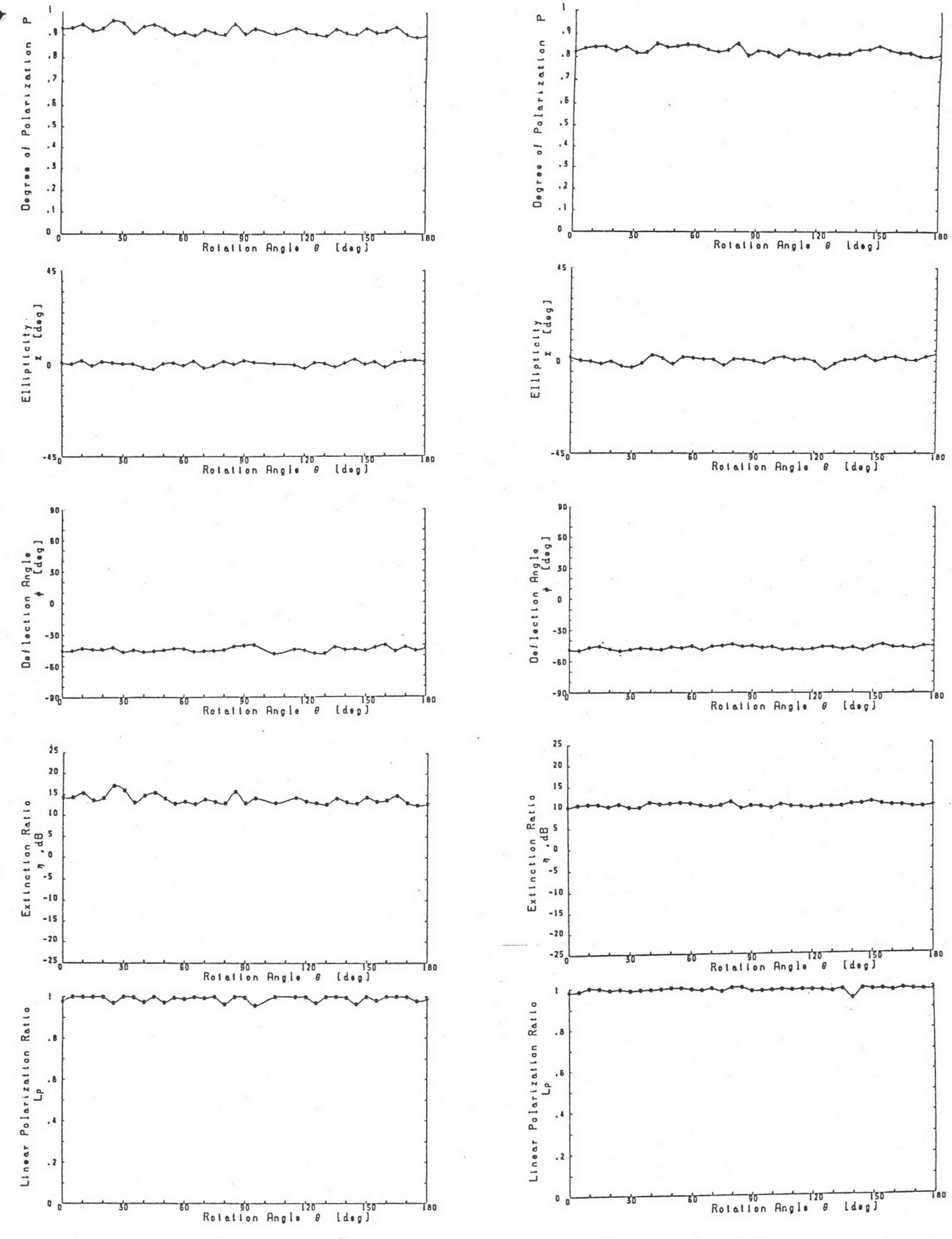

(a) (b)

Fig. 33. Polarization characteristics of the polarization recombined light as a function of the BSC rotation angle : (a) fiber length, l = 1.5 km; (b) l = 27 km.

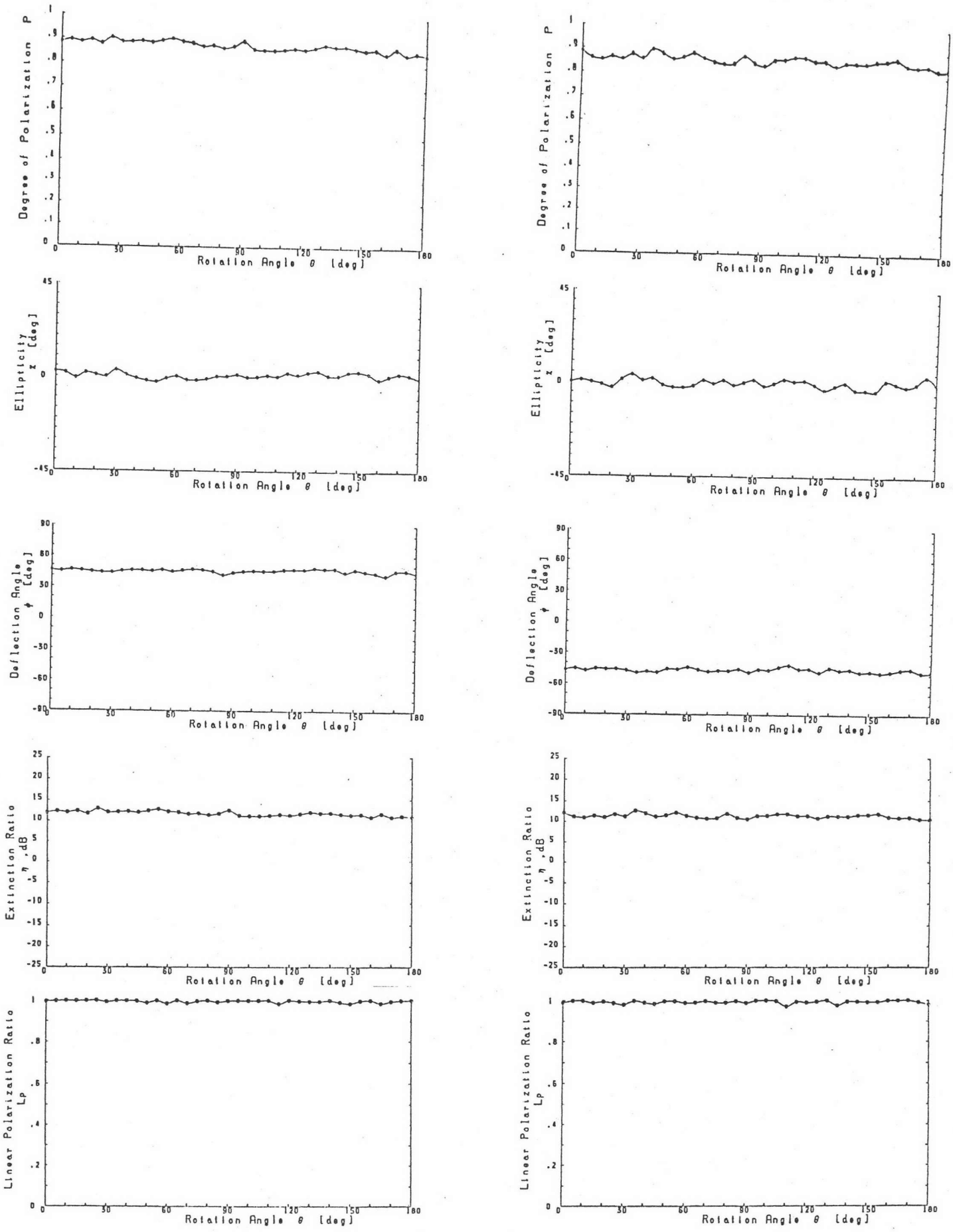

(a) (b)

Fig. 34. Polarization characteristics of the polarization recombined light as a function of the BSC for 15.4 km-long single-mode fiber : (a) the vertical V: polarization phase was rotated by 90° ; (b) the horizontal H: polarization phane was rotated by 90°.

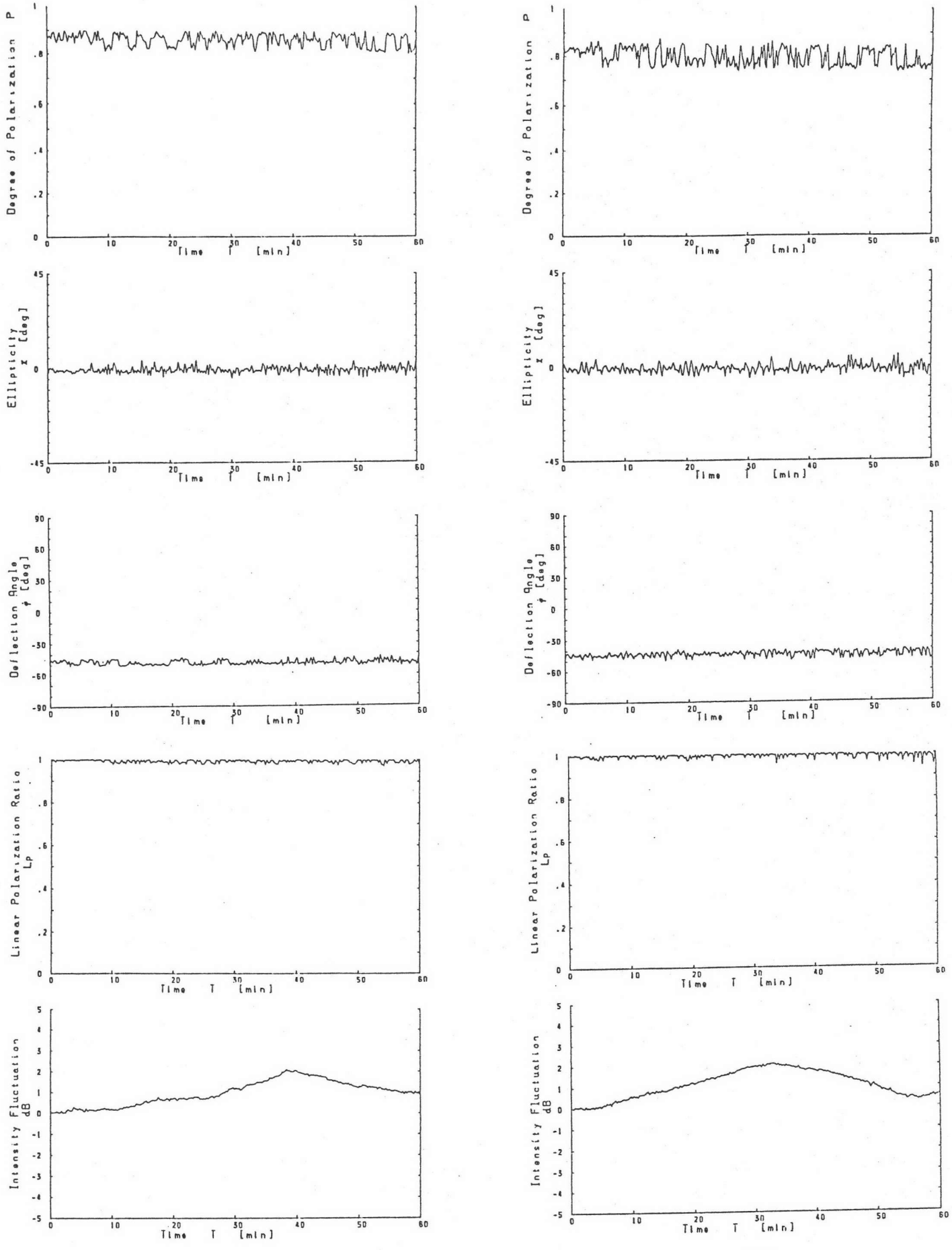

(a) (b)

Fig.35. Polarization characteristics, and intensity fluctuation relative to the initial value at T = 0: (a) l = 15.4 km; (b) l = 27 km.

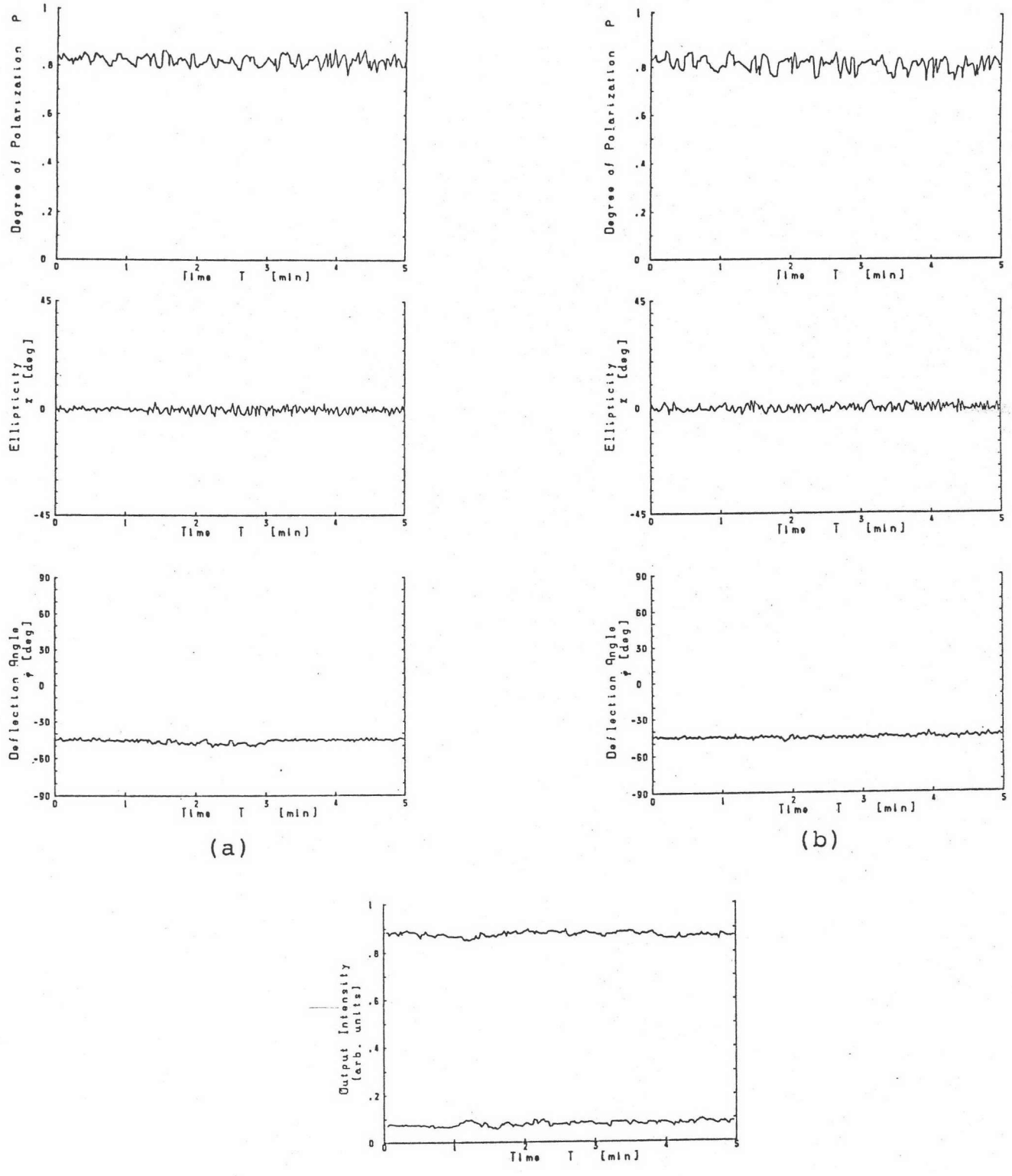

Fig. 36. Polarization characteristics of the polarization recombined light as a function of time for 27 km-long single-mode fiber. (a) output-1, (b) output-2, (c) maximum intensity at output 1 (upper trace), and minimum intensity at output 2 (lower trace).

one set of the four Strokes' parameters. Therefore, the light source fluctuation could cause variation in each of the four parameters for one set of measurement.

4.4. Summary

It has been shown that the SOP of the polarization recombined light is always linear with a fixed inclination (or deflection) angle (45° in this setup) regardless of the changes in the SOP of the incoming light. The extinction ratio was found to be 23 dB and a high DOP (= 0.82) was preserved in the 27-km test fiber. Despite the variations caused by the measuring system and optical components including environmental changes, the SOP in the polarization recombining light was stable and polarization fluctuation was slow.